

Case studies of atomic properties using coupled-cluster and unitary coupled-cluster methods

Chiranjib Sur , Rajat K. Chaudhuri, B. P. Das

NAPP Group, Indian Institute of Astrophysics, Bangalore 560 034, India

D. Mukherjee

Indian Association for the Cultivation of Science, Kolkata - 700 032, India

14th November 2018

Abstract

The magnetic dipole and electric quadrupole hyperfine constants of Aluminium (^{27}Al) atom are computed using the relativistic coupled cluster (CC) and unitary coupled cluster (UCC) methods. Effects of electron correlations are investigated using different levels of CC approximations and truncation schemes. The ionization potentials, excitation energies, transition probabilities, oscillator strengths and nuclear quadrupole moment are computed to assess the accuracy of these schemes. The nuclear quadrupole moment obtained from the present CC and UCC calculations in the singles and doubles approximations are 142.5 mbarn and 141.5 mbarn respectively. The discrepancies between our calculated IPs and EEs and their measured values are better than 0.3%. The other one-electron properties reported here are also in excellent agreement with the measurements.

PACS number(s) : 31.15.Ar, 31.15.Dv, 31.25.Jf, 32.10.Fn

1 Introduction

Theoretical studies of properties like hyperfine coupling constants and transition probabilities are stringent tests of the accuracies of atomic wave functions. The former is sensitive to the nuclear region while the latter crucially depends on the wavefunctions at large distances. High precision calculations of these properties require a rigorous incorporation of correlation effects [1] and in some cases even relativistic effects. In particular, the hyperfine coupling constants and transition electric dipole ($E1$) moments calculations are relevant to the studies of parity non-conservation (PNC) in atoms as PNC transition amplitudes involve both short range electro-weak interaction and $E1$ transition moments [2].

The relativistic and electron correlation effects can be incorporated in many-electron systems through a variety of many-body methods. Among these approaches, the relativistic coupled cluster (RCC) method has emerged as one of the most powerful and effective tool for a high precision description of electron correlations in many-electron systems [3]. Coupled-cluster (CC) is an all-order non-perturbative theory, and therefore, the higher order electron correlation effects can be incorporated more efficiently than using the order-by-order diagrammatic many-body perturbation theory (MBPT) [4]. The CC method is size-extensive [5], a property which has been found to be crucial for an accurate determination of state energies, bond cleavage energies for molecules and related spectroscopic constants. Since the order-by-order MBPT expansion terms are directly related to the terms in the CC wavefunction (as the latter is an all-order version of the former scheme), the CC results can be improved by adding certain important omitted diagrams by computing the corresponding low order MBPT diagrams to all order.

In this paper, we report our calculations of the magnetic dipole and electric quadrupole hyperfine constants (A and B respectively) for the lowest two $^2P_{3/2}$ states ($3^2P_{3/2}$ and $4^2P_{3/2}$) of ^{27}Al obtained using the RCC method. We also present ionization potentials (IPs), transition energies (EEs), transition probabilities and oscillator strengths of ^{27}Al . Effects of electron correlations on these quantities are investigated using different levels of CC approximation. We compare atomic properties of ^{27}Al obtained from CC and UCC methods to assess the relative performance and accuracy of these two schemes. The UCC and its variants [6, 7, 8, 9] were developed almost two decades ago to incorporate higher order electron correlation effect systematically. Recently we have applied the relativistic UCC to atomic systems for the first time to calculate properties like lifetime of excited states [10]. To our knowledge, no prior UCC calculations are available for ^{27}Al .

The nuclear quadrupole moment (Q) of ^{27}Al is of interest in several research areas [11]. The electric quadrupole hyperfine constant (B) of ^{27}Al was measured in ionic crystals [12, 13] and in metallic alloys [14] and the value of Q is extracted by combining the calculated electric field gradient (q) at the nucleus with the measured value of B . Q is also obtained from studying AlF and AlCl molecules [15]. Pernpointner and Visscher [16] have obtained the value of Q for Al , by studying AlF , AlCl and AlBr molecules using fully relativistic CCSD(T) theory. The value of Q is also obtained from the muonic x-ray [17, 18] and nuclear scattering experiments [19].

In 1976, Rogers *et al* [20] employed the second order MBPT method to determine the nuclear quadrupole moment Q of ^{27}Al . Later, Sundholm and Olsen [21] calculated Q for the $^2P_{3/2}$ state of Al using the multi-configuration Hartree-Fock (MCHF) approach [22]. Nuclear structure calculations of Q have also been carried out [23, 24, 25, 26]. The discrepancies between the calculated and measured values of Q suggest that inclusion of higher order electron correlation effects is necessary to improve the existing calculations. Our present work is motivated by this consideration. In this work, we have compared our calculated Q value of the with all the available calculated and measured values.

Section 2 briefly reviews the CC method. Computational details and results are discussed in the subsequent sections 3 and 4 respectively. Finally in the last section we highlight the findings of our work.

2 Methodology

Since the coupled cluster methods used in this work are discussed elsewhere [6, 7, 8, 9, 27, 28] in details, we only outline the essential features of the method here.

In this work, we employ the straight forward extension of non-relativistic coupled cluster theory to the relativistic regime by adopting the no-virtual-pair approximation (NVPA) along with appropriate modification of orbital form and potential terms [29]. We begin with Dirac-Coulomb Hamiltonian (H) which is expressed as

$$H = \sum_{i=1}^N [c\vec{\alpha}_i \cdot \vec{p}_i + \beta mc^2 + V_N(r_i)] + \sum_{i<j}^N \frac{e^2}{r_{ij}}. \quad (1)$$

The normal order form of the above Hamiltonian is given by

$$H = H_N - \langle 0|H|0 \rangle = \sum_{ij} \langle i|f|j \rangle \{a_i^\dagger a_j\} + \frac{1}{4} \sum_{i,j,k,l} \langle ij||kl \rangle \{a_i^\dagger a_j^\dagger a_l a_k\}, \quad (2)$$

where

$$\langle ij||kl \rangle = \langle ij|\frac{1}{r_{12}}|kl \rangle - \langle ij|\frac{1}{r_{12}}|lk \rangle. \quad (3)$$

The valence universal Fock space open-shell coupled cluster method is employed which begins with the decomposition of the full many-electron Hilbert space of dimension N into into a reference space \mathcal{M}_0 of dimension $M \ll N$, defined by the projector P , and its orthogonal complement \mathcal{M}_0^\perp associated with the projector $Q = 1 - P$. A valence universal wave operator Ω is then introduced which satisfies

$$|\Psi_i\rangle = \Omega|\Psi_i^{(0)}\rangle, \quad i = 1, \dots, M \quad (4)$$

where $|\Psi_i^{(0)}\rangle$ and $|\Psi_i\rangle$ are the *unperturbed* and *the exact* wave functions of the i th eigenstate of the Hamiltonian, respectively. The wave operator Ω , which formally represents the mapping of the reference space \mathcal{M}_0 onto the target space \mathcal{M} spanned by the M eigenstates $|\Psi_i\rangle$, has the properties

$$\Omega P = \Omega, \quad P\Omega = P, \quad \Omega^2 = \Omega. \quad (5)$$

With the aid of the wave operator Ω , the Schrödinger equation for the M eigenstates of the Hamiltonian correlating with the M -dimensional reference space, i.e.,

$$H|\Psi_i\rangle = E_i|\Psi_i\rangle, \quad i = 1, \dots, M, \quad (6)$$

is transformed into a generalized Bloch equation,

$$H\Omega P = \Omega H\Omega P = \Omega P H_{\text{eff}} P, \quad (7)$$

where $H_{\text{eff}} \equiv PH\Omega P$ is the effective Hamiltonian. Once Eq. (7) is solved for the wave operator Ω , the energies E_i , $i = 1, \dots, M$, are computed by diagonalizing the effective Hamiltonian H_{eff} in the M -dimensional reference space \mathcal{M}_0 . Following Lindgren's formulation of open-shell CC [27], we express the valence universal wave operator Ω as

$$\Omega = \{\exp(\sigma)\}, \quad (8)$$

and σ being the excitation operator and curly brackets denote the normal ordering.

The operator σ has two parts, one corresponds to the core sector and the other to the valence sector. In the coupled-cluster singles and double (CCSD) excitation approximation the excitation operator for the core sector is given by

$$T = T_1 + T_2 = \sum_{ap} \{a_p^\dagger a_a\} t_a^p + \frac{1}{2} \sum_{abpq} \{a_p^\dagger a_q^\dagger a_b a_a\} t_{ab}^{pq}, \quad (9)$$

t_a^p and t_{ab}^{pq} being the amplitude corresponding to single and double excitations respectively. In UCC theory the core excitation operator has a unitary form and is represented as $T - T^\dagger$. For a single valence system the excitation operator the valence sector turns out to be $\exp(S) = \{1 + S\}$ and

$$S_k = S_{1k} + S_{2k} = \sum_{k \neq p} \{a_p^\dagger a_k\} s_k^p + \sum_{bpq} \{a_p^\dagger a_q^\dagger a_b a_k\} s_{kb}^{pq}, \quad (10)$$

where s_k^p and s_{kb}^{pq} denotes the single and double excitation amplitudes for the valence sectors respectively. In Eqs. (9) and (10) we denote the core (virtual) orbitals by a, b, c, \dots (p, q, r, \dots) respectively and v corresponds to the valence orbital. In the unitary counterpart of CCSD, *i.e.* in UCCSD, since the core excitation operator also contains a de-excitation part (denoted by T^\dagger) it can be shown that for a given approximation the UCC theory contains certain higher excitations effects which is not present in the CC theory [10].

2.1 Computation of one-electron properties

We now present the method for computing the matrix-element of sum of one-body operator $O = \sum_{i=1}^N o_i$ that utilizes the structure $\Omega = \{\exp(\sigma)\}$. In this approach, the CC-equations are first solved to determine the σ cluster amplitudes and then the matrix-element of a one-body operator is computed through the following relation:

$$O_{fi} = \frac{\langle \Psi_f | O | \Psi_i \rangle}{\sqrt{\langle \Psi_f | \Psi_f \rangle} \sqrt{\langle \Psi_i | \Psi_i \rangle}}, \quad (11)$$

where $|\Psi_k\rangle$ denotes the exact k -th state wave-functions. It can be shown that the substitution of the expression for the exact wave-functions $|\Psi_i\rangle$ and $|\Psi_f\rangle$ in Eq.(11) explicitly cancels out spurious disconnected terms from the above expression which reduces to

$$O_{fi} = \frac{\langle \Psi_f | O | \Psi_i \rangle_c}{\sqrt{\langle \Psi_f | \Psi_f \rangle_c} \sqrt{\langle \Psi_i | \Psi_i \rangle_c}}, \quad (12)$$

where subscript c refers to the 'connected' terms.

2.2 Magnetic dipole and electric quadrupole hyperfine constants

The interaction between the various moments of the nucleus and the electrons of an atom are collectively referred to as hyperfine interactions [4]. Here we will briefly present and outline of the the magnetic dipole (A), electric quadrupole (B) hyperfine constants and the nuclear quadrupole moment (Q).

For a state $|IJFM_F\rangle$ the magnetic dipole hyperfine constant A is defined as

$$A = \mu_N \left(\frac{\mu_I}{I} \right) \frac{\langle J || T^{(1)} || J \rangle}{\sqrt{J(J+1)(2J+1)}}, \quad (13)$$

where μ_I is the nuclear dipole moment defined in units of Bohr magneton μ_N ; \mathbf{I} and \mathbf{J} are the total angular momentum for the nucleus and the electron state respectively and $\mathbf{F} = \mathbf{I} + \mathbf{J}$ with the projection M_F . The electric quadrupole hyperfine constant B for the same state is defined as

$$B = 2eQ \left[\frac{2J(2J-1)}{(2J+1)(2J+2)(2J+3)} \right]^{1/2} \langle J \| T^{(2)} \| J \rangle, \quad (14)$$

where Q denotes the nuclear quadrupole moment.

The single particle forms ($t^{(k)}$) of the operator $T^{(k)}$ ($k = 1, 2$) are taken from Cheng's paper [30] and are represented as

$$T_q^{(1)} = \sum_q t_q^{(1)} = \sum_j -ie \sqrt{\frac{8\pi}{3}} r_j^{-2} \vec{\alpha}_j \cdot \mathbf{Y}_{1q}^{(0)}(\hat{r}_j) \quad (15)$$

and

$$T_q^{(2)} = \sum_q t_q^{(2)} = \sum_j -er_j^{-3} C_q^{(2)}(\hat{r}_j). \quad (16)$$

Here $\vec{\alpha}$ is the Dirac matrix and \mathbf{Y}_{kq}^λ is the vector spherical harmonics and $C_q^{(k)} = \sqrt{\frac{4\pi}{(2k+1)}} Y_{kq}$. In Eq.(15) the index j refers to the j -th electron of the atom and e is the magnitude of the electronic charge.

2.3 Electric dipole transition probabilities and oscillator strengths

The transition probability $A_{f \leftarrow i}$ (in sec^{-1}) and oscillator strength f_{if} (in a.u.) for the electric dipole allowed transitions are given by [31]

$$A_{f \leftarrow i} = \frac{2.0261 \times 10^{18}}{g_f \lambda^3} S_{f \leftarrow i} \quad (17)$$

and

$$f_{if} = 1.499 \times 10^{-16} \frac{g_f}{g_i} \lambda^2 A_{f \leftarrow i} \quad (18)$$

respectively. Here, λ is the wave length in \AA and $g_f(g_i) \equiv (2J+1)$ is degeneracy of the upper (lower) level. The quantity $S_{f \leftarrow i}$ is the $E1$ line strengths (in atomic units), respectively. The line strengths $S_{f \leftarrow i}$ is defined as

$$S_{f \leftarrow i} = D_{if} \times D_{fi}, \quad (19)$$

where the electric dipole D_{fi} matrix elements is given by

$$D_{fi} = C(f, i) \int dr [P_f(r)P_i(r) + Q_f(r)Q_i(r)] r, \quad (20)$$

with

$$C(f, i) = (-1)^{j_f+1/2} \begin{pmatrix} j_f & 1 & j_i \\ 1/2 & 0 & -1/2 \end{pmatrix} \sqrt{(2j_f+1)(2j_i+1)}. \quad (21)$$

3 Computational Details

The Fock-space relativistic coupled cluster method is applied to compute the ground and excited state energies of Al . The Dirac-Fock equations are first solved for the alkali metal ion M^+ , which defines the (0-hole,0-particle) sector of the Fock space. The ion is then correlated using the closed shell CCSD/LCCSD, after which one-electron is added following the Fock-space scheme

$$M^+(0, 0) \longrightarrow M^+(0, 1).$$

Here LCCSD corresponds to linearized coupled-cluster in singles and doubles. Both the DF and relativistic CC programs utilize the angular momentum decomposition of the wave-functions and CC equations. Using the Jucys- Levinson-Vanagas (JLV) theorem [32], the Goldstone diagrams are expressed as a products of angular momentum diagrams and reduced matrix element. This procedure simplifies the

computational complexity of the DF and relativistic CC equations. We use the kinetic balance condition to avoid the “variational collapse” [33].

In the actual computation, the DF ground state and excited state properties of *Al* are computed using the finite basis set expansion method (FBSE) [34] with a large basis set of (32s28p24d15f) Gaussian functions of the form

$$F_{i,k}(r) = r^k \cdot e^{-\alpha_i r^2} \quad (22)$$

with $k = 0, 1, \dots$ for s, p, \dots type functions, respectively. For the exponents, the even tempering condition

$$\alpha_i = \alpha_0 \beta^{i-1} \quad (23)$$

is applied. Here, N is the number of basis functions for a specific symmetry. The self-consistent DF orbitals are stored on a grid. It is assumed that virtual orbitals with high energies do not contribute significantly to properties like IPs. In the CCSD calculations, we therefore truncate the virtual s, p, d and f orbitals above 1000 a.u., 1000 a.u., 500 a.u. and 100 a.u., respectively. Single and double excitations from all the core orbitals to valence or virtual orbitals are considered.

Table 1: Transition energies (in cm^{-1}) of *Al* atom. IP is the ionization potential, EE denotes the excitation energies with respect to the $^2P_{1/2}$ ground state.

	Dominant Configuration	State	LCCSD	CCSD	UCCSD	Expt[35]
IP	[Mg]3p _{1/2}	$^2P_{1/2}$	48194.92	48155.42	48211.83	48279.16
EE	[Mg]3p _{3/2}	$^2P_{3/2}$	133.94	114.75	114.55	112.04
	[Mg]4s _{1/2}	$^2S_{1/2}$	24802.66	24937.55	24988.00	25347.69
	[Mg]4p _{1/2}	$^2P_{1/2}$	32464.50	32521.12	32572.34	32949.84
	[Mg]4p _{3/2}	$^2P_{3/2}$	32481.26	32537.68	32588.94	32965.67

4 Results and Discussions

Table 1 compares the IP and EE of *Al* computed using different CC methods with the experiment [35]. It can be seen from this table that UCCSD calculations of the IP and EEs are more accurate than the CCSD and LCCSD results. Although not well understood, the present as well as some earlier studies [1] indicate that the IPs computed using the LCCSD scheme are sometimes in better agreement with the experiments than the corresponding CCSD calculations. For instance, the $^2P_{1/2}(3p_{1/2})$ IP estimated using LCCSD method differs by 84 cm^{-1} from the measured value, while the corresponding CC value is off by 124 cm^{-1} . However, it is clear from Table 1 that CCSD estimates the EE more accurately than the LCCSD scheme for the low lying states.

In table 2 we present the results of our nuclear quadrupole moment (Q) calculation using different CC methods with other calculations [20, 21] and different measurements [15, 17, 18, 19]. Pyykkö has reviewed, calculated and measured Q values for a number of systems [11]. Comparison of our results with the existing data will give an indication of the potential of the CC and UCC methods to provide accurate estimate of nuclear properties. It is evident from table 2 that Q calculated using the second order MBPT calculations by Rogers *et al.* [20] is far outside the experimental limits whereas the value obtained by the restricted active space (RAS) based multi-configuration Hartree-Fock (MCHF) [22] calculation is closer to the experimental limits. The uncertainty in molecular experiment is less compared to the muonic experiments. Although our CC and UCC results are slightly outside the experimental limits, they could be of some importance in determining the accurate value of Q from a wide range of values.

The MBPT(2) and MCHF results clearly indicate that the contributions from non linear terms present in CC and UCC theories are non-negligible and this is further supported by the results of our different CC calculations of Q . The extremely accurate estimate of Q offered by LCCSD scheme is perhaps a bit fortuitous. Nevertheless, the performance of CC, especially the UCC, outshines the MBPT(2) and MCHF treatments. Note that the effects of partial triple and quadrupole excitations are present in

Table 2: Comparison of the nuclear quadrupole moments Q (in mbarn) of ^{27}Al estimated using various CC approach with the experiment and with other theoretical calculations.

Method	Q
LCCSD	146.7
CCSD	142.5
UCCSD	141.5
MBPT(2)[20]	165(2)
MCHF[22]	140.3(1.0)
Molecular Exp[15]	146.6(1.0)
Molecular Theory [16]	146.0(4)
Muonic Exp.[17, 18]	150(6)
Nuclear Scattering[19]	155(3)
Nuclear Theory[23, 24]	134
Nuclear Theory[24, 25]	150.8
Nuclear Theory[25, 26]	138.9

our UCC calculations. The CC and UCC theories unlike the MCHF method are size-consistent and incorporate certain higher order excitations that the MCHF does not at the same level of approximation. For example, at the level of single and double (SD) excitations, the CC theory includes not only the effect of T_2 but also T_2^2 ; whereas the effect of T_2^2 can be obtained in MCHF only if one considers the quadrupole excitations. Also, that calculation is non-relativistic with a relativistic correction added while our calculation is fully relativistic.

Table 3: Magnetic dipole hyperfine (A) matrix elements (in MHz) of Al atom.

Method	$A(3p_{1/2})$	$A(3p_{3/2})$	$A(4s_{1/2})$	$A(4p_{1/2})$	$A(4p_{3/2})$
LCCSD	493.30	108.39	414.14	55.97	26.26
CCSD	498.06	101.49	405.94	58.32	23.09
UCCSD	498.33	100.98	407.18	58.28	23.12
Expt [36]	502.0346(5)	94.27723(10)			

The values of A for the ground and excited states of Al computed using the LCCSD, CCSD and UCCSD methods are displayed in Table 3. Our calculated values of A agrees well with the experimental values [36] for the $^2P_{1/2}(3p_{1/2})$ and $^2P_{3/2}(3p_{3/2})$ state. We also present the values of A for some other low lying states which could be useful for experimentalists. We have also computed the electric quadrupole hyperfine constant (B) for two low lying $^2P_{3/2}(3p_{3/2})$ and $(4p_{3/2})$ states using CCSD(UCCSD) theory which are respectively 19.49 MHz(19.59 MHz) and 2.85 MHz(2.86 MHz) whereas the experimental value of B for the $^2P_{3/2}(3p_{3/2})$ state is 18.915 MHz [37, 38].

In Table 4, we compare the $3p_{1/2} \rightarrow 4s$ and $3p_{3/2} \rightarrow 3s$ wave lengths (λ), oscillator strengths (f_{ik}), line strengths (S_{ik}) and transition probabilities (A_{ik}) obtained from LCCSD, CCSD and UCC schemes with the experiment. Table 4 shows that our computed quantities (λ , S_{ik} , and A_{ik}) are in excellent agreement with experiment especially those predicted by the UCC scheme. That this scheme provides more accurate estimates of IP, EE etc. and is also evident from Figure 1, where the absolute errors (in %) in the computed properties are plotted against different CC schemes.

5 Conclusion

The relativistic open-shell coupled cluster scheme for direct energy difference calculations and several one electron properties is presented and applied to Al . In this work, we investigate the effects of electron correlations on the ground and excited state properties using different levels of CC approximations. We

Table 4: Wave lengths λ (in Å), line strengths $S_{ik} \equiv |r|^2/a_0^2$ (in a.u.), transition probabilities A_{ik} (in $10^8 s^{-1}$), and oscillator strengths f_{ik} (in a.u.) for $[\text{Mg}]3p \rightarrow [\text{Mg}]4s$ transitions of Al atom.

Method	$[\text{Mg}]3p_{1/2} \rightarrow 4s$				$[\text{Mg}]3p_{3/2} \rightarrow 4s$			
	λ	S_{ik}	A_{ik}	f_{ik}	λ	S_{ik}	A_{ik}	f_{ik}
LCCSD	4031.82	3.379	0.522	0.127	4053.72	6.763	1.028	0.127
CCSD	4010.05	3.292	0.517	0.125	4028.59	6.634	1.028	0.125
UCCSD	4001.92	3.275	0.517	0.114	4020.35	6.600	1.029	0.125
Expt[39]	3944.01	2.99	0.493	0.115	3961.52	6.0	0.98	0.115

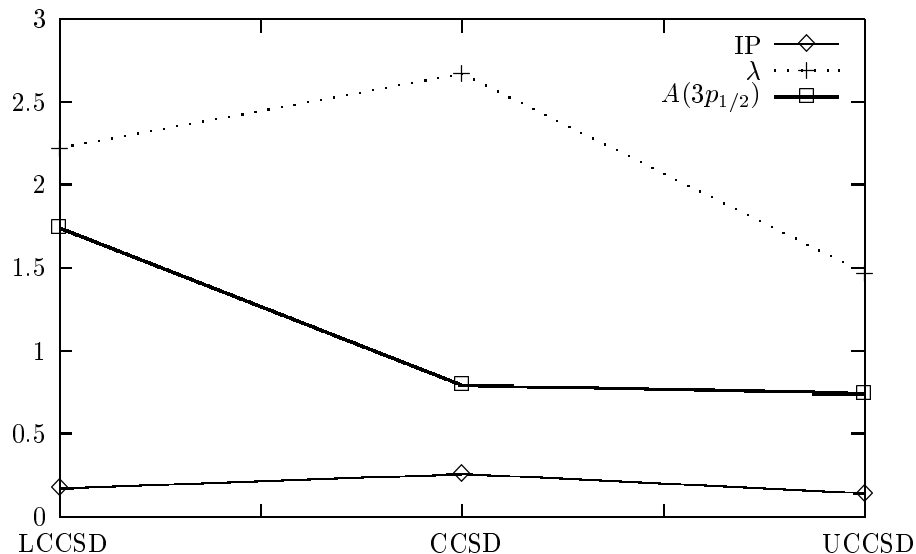


Figure 1: Absolute error (in %) of the computed IP, $^2P_{1/2}(3p_{1/2}) \rightarrow ^2S_{1/2}(4s)$ wave lengths (λ), magnetic dipole hyperfine constant (A) for the $3p^2P_{1/2}$ state using different CC methods.

have shown that unitary coupled cluster (UCC) method is capable of providing accurate estimates of wave lengths, transition probabilities, oscillator strengths, nuclear quadrupole moment, magnetic dipole and electric quadrupole hyperfine constants for relatively light atomic systems with a single valence electron. The calculated value of Q compared to others are closer to the experimental uncertainties than all the existing atomic and nuclear calculations, thereby demonstrating that RCC theory of atoms can yield accurate values of nuclear quadrupole moments. Such an inter-disciplinary approach involving atomic and nuclear physics adds a new dimension to this theory.

Acknowledgments : One of the authors (CS) acknowledges the BRNS for project no. 2002/37/12/BRNS.

References

- [1] R. K. Chaudhuri, B. K. Sahoo, B. P. Das, H. Merlitz, U. S. Mahapatra and D. Mukherjee, *J. Chem. Phys.*, 119, 10633 (2003).
- [2] J. S. M. Ginges and V. V. Flambaum, *Phys. Rep.*, **397**, 63 (2004).
- [3] U. Kaldor, *Recent Advances in Coupled-Cluster Methods*, p 125, Ed. Rodney J. Bartlett, World Scientific, Singapore (1997).
- [4] I. Lindgren and J. Morrison, *Atomic Many-Body Theory*, Springer, Berlin (1985).

- [5] R. F. Bishop, *Lecture Notes in Physics, Microscopic Quantum Many-Body Theories and their Applications*, p.1, Eds. J. Navarro and A. Polls, Springer-Verlag-Berlin, Heidelberg and New York (1998).
- [6] W. Kutzelnigg, *J. Chem. Phys.*, **77**, 3082 (1982).
ibid, **80**, 882(1984).
- [7] S. Pal, M. D. Prasad and D. Mukherjee, *Theor. Chim. Acta*, **62**, 523 (1983).
- [8] S. Pal, *Theor. Chim. Acta*, **66**, 207 (1984).
- [9] J. D. Watts, G. W. Trucks and R. J. Bartlett, *Chem. Phys. Lett.*, **157**, 359 (1989).
- [10] C. Sur, B. K. Sahoo, R. K. Chaudhuri, B. P. Das and D. Mukherjee, *arxiv : physics/0502033*.
- [11] P. Pyykkö, *Mol. Phys.*, **99**, 1617 (2001).
- [12] R. V. Pound, *Phys. Rev.*, **79**, 689 (1950).
- [13] P. F. Liao and S. R. Hartmann, *Phys. Rev. B*, **8**, 69 (1973).
- [14] Y. Fukai and K. Watanbe, *Phys. Rev. B*, **10**, 3015 (1950).
- [15] V. Kellö, A. J. Sadlej, P. Pyykkö, D. Sundholm and M. Tokman, *Chem. Phys. Lett.*, **304**, 414 (1999).
- [16] M. Pernpointner and L. Visscher, *J. Chem. Phys*, **114**, 10389 (2001).
- [17] R. Weber *et al.*, *Nucl. Phys. A*, **377**, 361 (1982).
- [18] R. Weber *et al.*, *Phys. Lett.*, **98B**, 343 (1981).
- [19] D. Schwalm, E. K. Warburton and J. B. Olness, *Nucl. Phys. A*, **293**, 425 (1977).
- [20] J. E. Rodgers, R. Roy and T. P. Das, *Phys. Rev. A*, **14**, 543 (1976).
- [21] D. Sundholm and J. Olsen, *Phys. Rev. Lett.*, **68**, 927 (1992).
- [22] D. Sundholm and J. Olsen, *Chem. Phys. Lett.*, **177**, 91 (1991) and references therein.
- [23] B. H. Wildenthal, J. B. McGrory and P. W. M. Glaudemans, *Phys. Rev. Lett.*, **26**, 96 (1971).
- [24] M. Carchidi, B. H. Wildenthal and B. A. Brown, *Phys. Rev. C*, **34**, 2280 (1986).
- [25] S. Krewald, K. W. Schmid and A. Fessler, *Z. Phys.*, **269**, 125 (1974).
- [26] B. A. Brown, W. Chung and B. H. Wildenthal, *Phys. Rev. C*, **22**, 774 (1980).
- [27] I. Lindgren, *Int. J. Quant. Chem.*, **S12**, 33 (1978).
- [28] D. Mukherjee and S. Pal, *Adv. Quant. Chem.*, **20**, 281 (1989).
- [29] E. Eliav, U. Kaldor and Y. Ishikawa, *Phys. Rev. A*, **50**, 1121 (1994).
- [30] K. T. Cheng and W. J. Child, *Phys. Rev. A*, **31**, 2775 (1995).
- [31] L. I. Sobelman, *Introduction to the Theory of Atomic Spectra*, Pergamon Press, Oxford, (1972).
- [32] A. P. Jucys (Yutsis), I. B. Levinson and V. V. Vanagas, *Mathematical Apparatus of the Theory of Angular Momentum*, Israel Program for Scientific Translation, Jerusalem (1962).
- [33] A. D. McLean and Y. S. Lee, *J. Chem. Phys.*, **76**, 735 (1982).
- [34] R. K. Chaudhuri, P. K. Panda and B. P. Das, *Phys. Rev. A*, **59**, 1187 (1999).
- [35] C. E. Moore, *Atomic Energy Levels, Natl. Bur. Stand. Ref. Data, U.S.*, Circ no. 35, vol 1, U.S. GPO, Washington, D. C. (1971).
- [36] J. M. Brown and K. M. Evenson, *Phys. Rev. A*, **60**, 956 (1999).

- [37] N. J. Martin, P. G. H. Sandars and H. Lew, *Proc. Roy. Soc.*, London, **A305**, 139 (1968).
- [38] J. S. M. Hervey, L. Evans and H. Lew, *Can. J. Phys.*, **1719**, 50 (1972).
- [39] Atomic Transition Probabilities, *Natl. Bur. Stand. Ref. Data, U. S.*, Circ no. 22, U.S. GPO, Washington, D. C. (1971).